

Supplemental Material for:

Pilot-scale groundwater monitoring network for earthquake surveillance and forecasting research in Korea

Hyun A. Lee ¹, Se-Yeong Hamm ², Nam C. Woo ^{1,3,*}

¹ Earth System Sciences Research Center, Yonsei University; hyunalee@yonsei.ac.kr

² Department of Geological Sciences, Pusan National University; hsy@pusan.ac.kr

³ Department of Earth System Sciences, Yonsei University; ncwoo@yonsei.ac.kr

* Correspondence: ncwoo@yonsei.ac.kr; Tel.: +82-2-2123-2674

This Supplementary Material contains three main sections:

Section 1: The supplementary information on the monitoring system;

Section 2: Well logging data obtained during the installation of MW2 - MW6;

Section 3: The results of harmonic analyses to identify the aquifer types; and

Section 4: The observational results of public monitoring networks between January 1, 2018 and February 28, 2018.

Section 1: The supplementary information on the monitoring system

This section provides the supplementary information on the monitoring system shown in following figures.

Once the data is sent to the server, a background program runs to input the data on the database and the internet server for data distribution, meanwhile checking failure of transmission. Then, another background program runs for analysis to identify abnormal changes. The analytical methods in this study are based on the displacement between observations: 1) displacement between water level at 24 hours before and current level; 2) ratio of level differences in a minute to the mean and standard deviation value of differences in a certain time frame; 3) comparison of water level with the moving averages of 1 day, 15 days, 30 days, and 90 days. Then, abnormal changes between level differences are also stored in the database.

The GW-EQ program was developed using C with MFC. The program provides the observed water level, and temperature or EC from the installation of the sensor to the end of data stored in the server. The precipitation data in the closest weather station is plotted at the top of the frame. The earthquake catalog is shown at the bottom if the user selected to check. If the earthquake is sufficiently large or close to the station with the concept of the effective radius by Dobrovolsky et al. (1979), the occurrence time of the earthquake is indicated as a red dashed line. And if co-seismic changes are expected in the well referring to Wang and Manga (2010), a blue dashed line appears.

The mobile application was also developed for alarming the transmission failure and abnormal changes found by automatic analysis as well as brief checks on the fluctuation. Through the application, we can see the station which is currently not operated or missed, while the abnormal changes are noticed as push alarm service. Currently, it supports only the Android operating system.

* Dobrovolsky, I.; Zubkov, S.; Miachkin, V. Estimation of the size of earthquake preparation zones. *Pure and applied geophysics* 1979, 117, 1025-1044.

* Wang, C.-Y.; Manga, M. Hydrologic responses to earthquakes and a general metric. *Geofluids* 2010, 10, 206-216, doi:<https://doi.org/10.1111/j.1468-8123.2009.00270.x>.

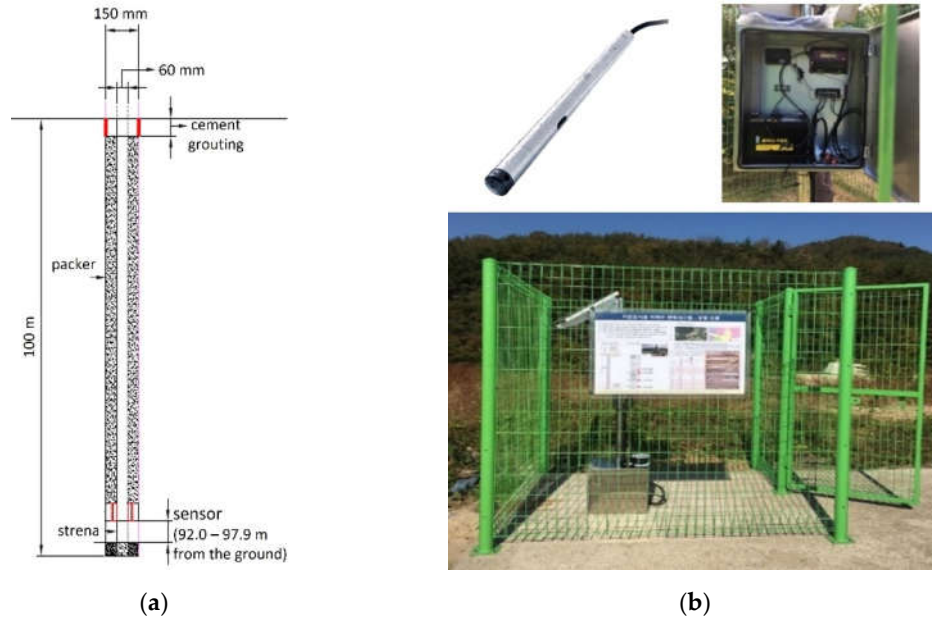


Figure S1. The groundwater monitoring system for surveillance of earthquake: (a) a schematic diagram of monitoring well structure (for example, MW2), and (b) the front view of the station. Pictures above the front view shows the monitoring sensor and the control box equipped at each station.

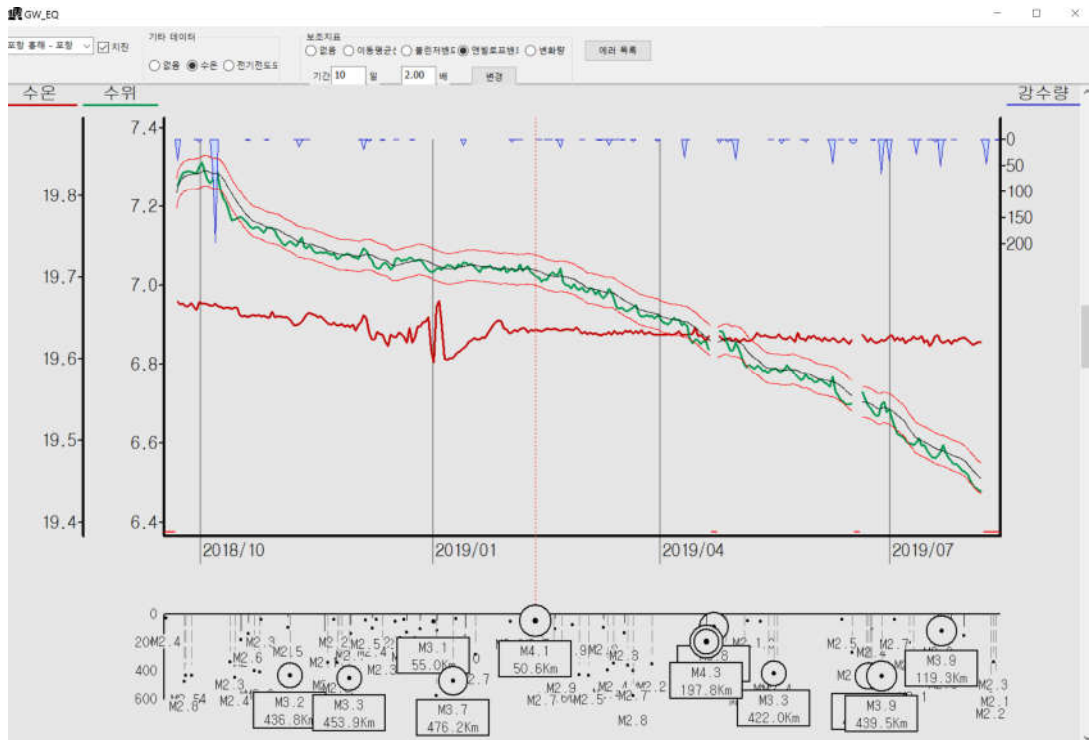


Figure S2. The interface of the GW-EQ program developed in this study (Displays are in Korean). The water-level (green line) and temperature (red line) or EC is shown in the main frame and the earthquake catalog is plotted in the bottom as the distance from epicenter and magnitude. The magnitude ≥ 3.0 earthquakes are highlighted with box. The vertical dashed line in red color indicates the precursor-expected events based on the effectiveness radius by Dobrovolsky et al. (1979).

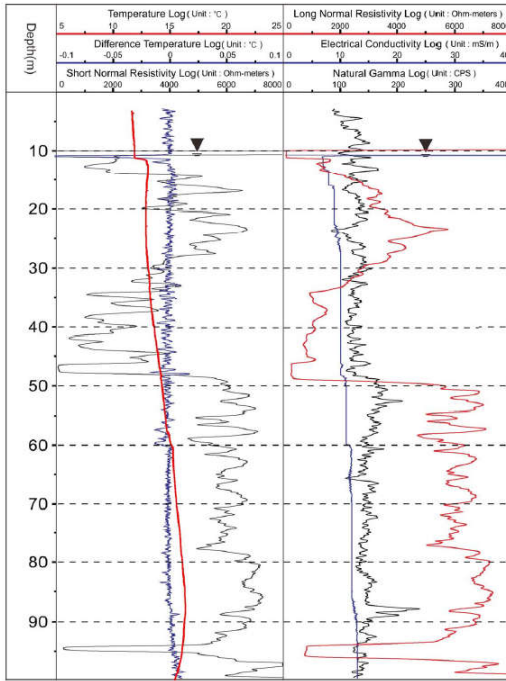


Figure S3. The typical screen of the mobile application developed in this study (Displays are in Korean): (a) the status of monitoring well, and (b) the water level fluctuation in a station with precipitation data. The green dot in (a) indicates that the monitoring station is normally in operation, meanwhile the red one means the data transmission is not recognized at the server.

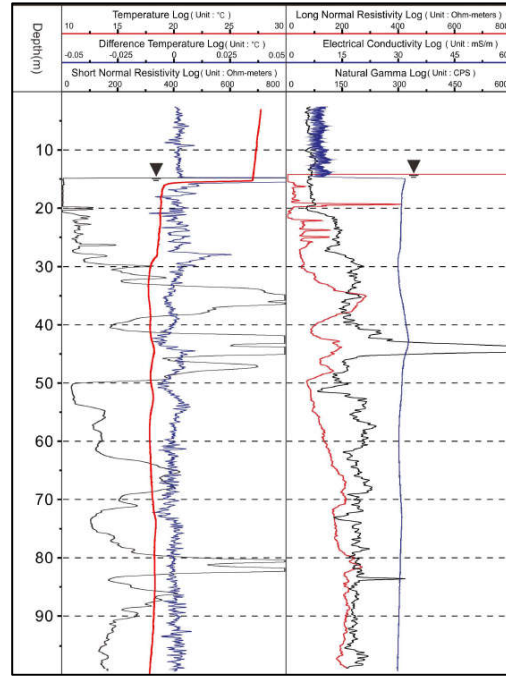
Section 2: Well logging data obtained during the installation of MW2 - MW6

This section includes the results of well logging during the installation of MW2 - MW6; the MW1 was installed in 2010, that before this study was initiated. In addition, the optical imaging was used to obtain images of borehole walls prior to the insertion of perforated and solid casing materials for station M1, MW3–MW7. In the MW2, the optic imaging was not used due to the difficulties in access.

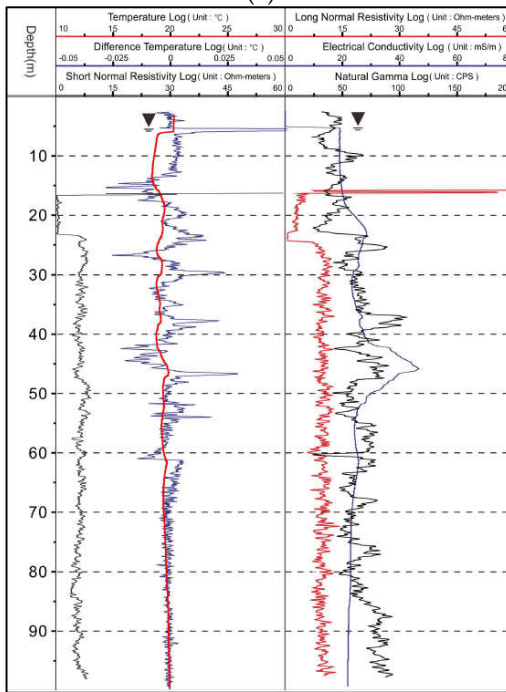
The logging methods includes electric resistivity, natural gamma rays, temperature, and electric conductivity (EC) tests. The electric resistivity logging measures the electric resistivity of strata near borehole. The logging method can be subdivided by the number and gap (i.e. spacing) of electrodes: normal resistivity log, lateral resistivity log, focused resistivity log, and micro resistivity log. In this study, the normal resistivity log with four electrodes was occupied. A set of current and potential electrodes were input to the borehole, while other set was connected to the ground surface. Through the logging, the apparent resistivity is primarily measured, then, the actual resistivity is estimated with calibration process. The natural gamma-ray logging records the intensity of gamma ray that released from the radioactive elements in rocks. Typical sources of the natural gamma-ray include potassium, radon, uranium, and thorium. The intensity of gamma ray is usually correlated with the contents of radioactive isotopes and mineralogy; therefore, it is used for the identification of rock types and salinity of water. On the other hand, the temperature and electric conductivity tests are used for detecting the depths of inflow and outflow. The temperature logging measures the vertical distribution of fluid temperature using the thermistor thermometer. If the electric current is applied to the thermistor thermometer, the thermometer can detect the resistivity changes induced by temperature changes. The temperature logger can respond to temperature of nearby fluid, thus, the measured temperature of fluid can be different from that of adjunct rocks. The electric conductivity test provides the information on the dissolved ions in the water. The EC meter measures the ability of water to pass the electric current when the water inflows to the electrode inside. The electrode is designed not to be influenced by other fluids or solids which is not contacted with, and subsequently, the borehole temperature cannot effect the results.



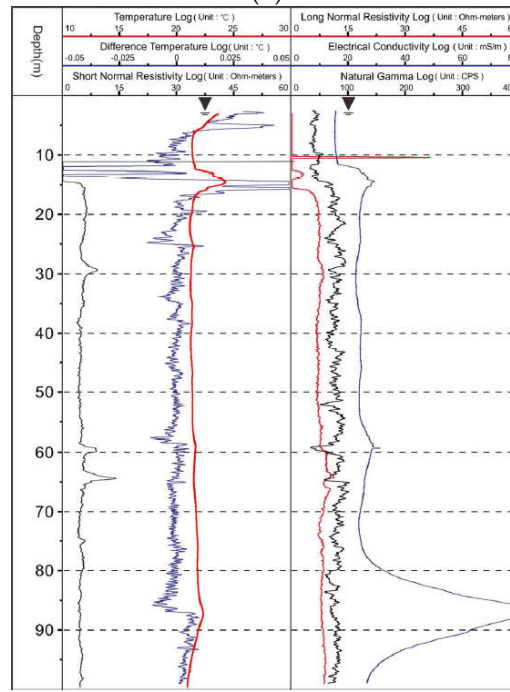
(a)



(b)



(c)



(d)

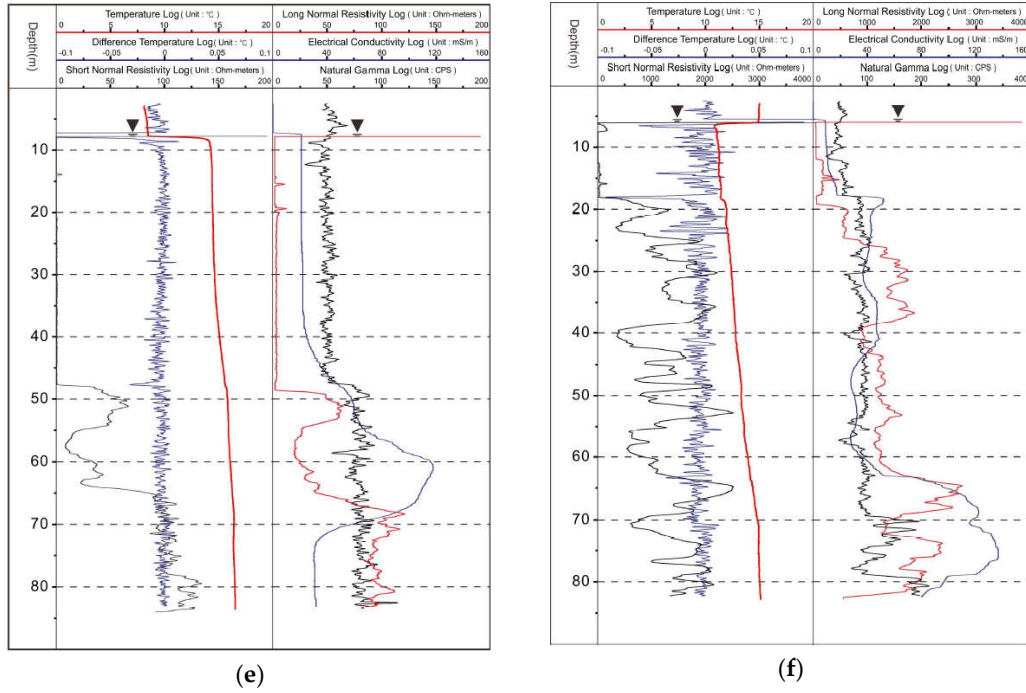


Figure S4. The results of well logging obtained from (a) MW2, (b) MW3, (c) MW4, (d) MW5, (e) MW6, and (f) MW7.

Table S1. The results of optic imaging observed at (a) MW1, (b) MW2, (c) MW3, (d) MW4.

(a) MW1

Analyzed depth	1.57 – 297.78 m	
Average Azimuth	N185.89	
Average Dip	47.27	
Fracture Counts	101	
Fracture Density	0.97 /m	
Mostly observed in	100 – 140 m, 160 – 180 m	

(b) MW2

Analyzed depth	3.67 - 96.69 m	
Average Azimuth	N68	
Average Dip	154	
Fracture Counts	101	
Fracture Density	0.97 /m	
Mostly observed in	0 – 10 m	

(c) MW3

Analyzed depth	1.57 – 98.94 m	
Average Azimuth	N220.78	
Average Dip	45.41	
Fracture Counts	107	
Fracture Density	1.37 /m	
Mostly observed in	30 – 50 m	

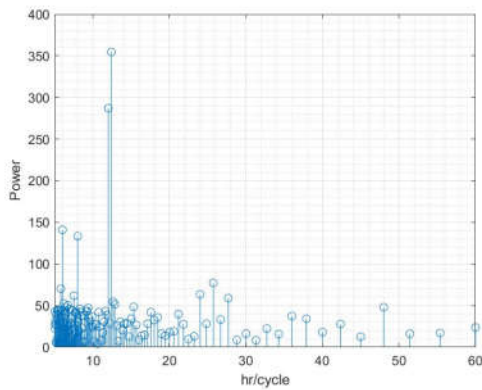
(d) MW4

Analyzed depth	1.57 – 61.12 m	
Average Azimuth	N146.02	
Average Dip	52.83	
Fracture Counts	28	
Fracture Density	0.76 /m	
Mostly observed in	30 – 44 m	

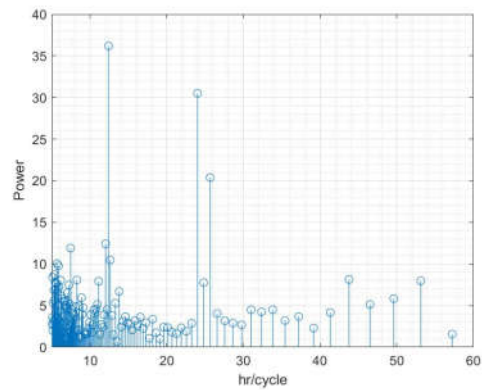
Section 3: The results of harmonic analyses to identify the aquifer types

This section includes the results of harmonic analyses which presented as the graphs in frequency domain. The analysis was conducted following Rahi and Halihan (2013) with exception of data interval; data with 15-minute interval was used for the original work, while this study used data with 1-minute interval.

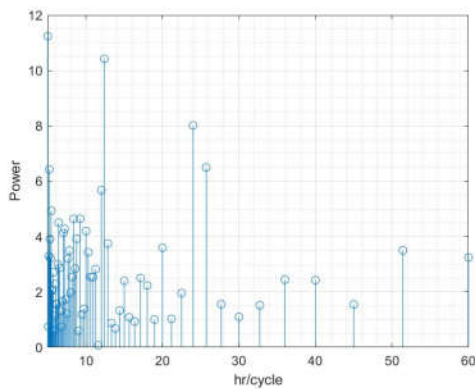
Of all tidal components, the principal lunar diurnal O1 (25.819 h), luni-solar diurnal K1 (23.934 h), principal lunar M2 (12.421 h), principal solar S2 (12.000 h), and larger lunar elliptic N2 (12.658 h) are considered significant for analyzing water level fluctuations. The aquifer type of each station was determined by comparing the power of each component.



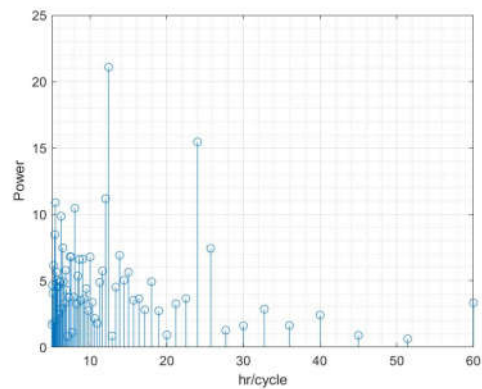
(a)



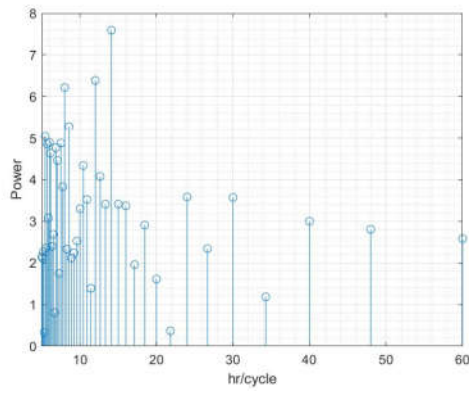
(b)



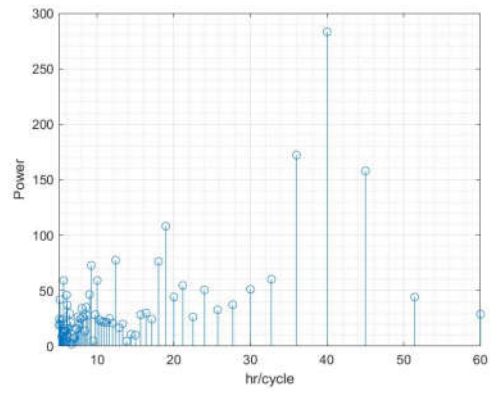
(c)



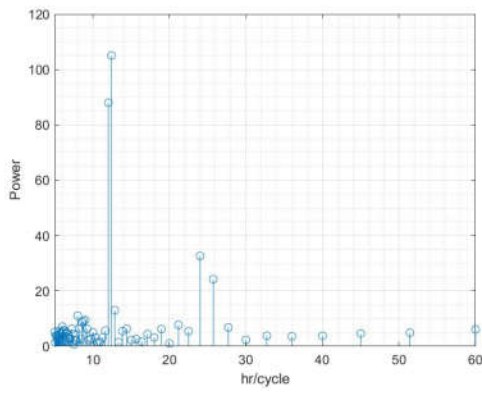
(d)



(e)



(f)



(g)

Figure S5. The results of harmonic analyses in frequency domain to identify the aquifer type: (a) MW1, (b) MW2, (c) MW3, (d) MW4, (e) MW5, (f) MW6, and (g) MW7.

Section 4: The observational results of public monitoring networks

This section includes the observational results of local groundwater monitoring stations along the Yangsan fault, and the National Groundwater Monitoring Network (NGMN) operated by K-water and Rural Groundwater Monitoring Network (RGMN) / Seawater Intrusion Monitoring Network (SIMN) of Korea Rural Community Corporation (KRCC) in Pohang during the M4.6 Pohang earthquake, which occurred on 05:03:03 February 11, 2018 (KST), the largest aftershock of 2017 M5.4 Pohang earthquake.

The local groundwater monitoring network is established as the supplementary public network of NGMN to provide the basic data on the water level and quality for water resources and contamination management (<http://www.gims.go.kr/>). A total of 2,793 stations are installed nationwide, and 47 monitoring stations are currently operated in Yangsan area. Out of 47 monitoring stations, three wells are closed to the MW1 monitoring well (Figure 1). The depth of boreholes, MG1, MG2, and MG3, are 120, 140, and 30 m, respectively, while that of MW1 is 300 m. The casing is established on each well to prevent inflow from the unconfined aquifers: 30 m for MG1 and MG2, and no data is provided for MG3.

On the other hand, the NGMN has been established since 1995 to monitor the regional groundwater situation and to provide the basic information of the groundwater in Korea according to the Groundwater Act of Korea. Each of the stations was designed to have two monitoring wells for the deep bedrock aquifer and the shallow alluvial aquifer, having three screen sections. However, a fair number of the station has the only bedrock monitoring-well due to the thin alluvial layer. The depth of wells for the bedrock and alluvial aquifer generally ranges 50 - 60 m and 10 - 20 m, respectively. The wells are equipped with the automatic data-logger which records the water level, temperature, and electric conductivity (EC) every hour; the barometric effect is calibrated at the same time using the embedded sensor. The collected data are sent once a day to the National Groundwater Information Management and Service Center (GIMS) through the remote terminal unit. In February 2018, six stations were operated in Pohang.

RGMN and SIMN have been established to manage the groundwater resource in the rural and coastal areas, respectively. Therefore, the metropolitan cities such as Seoul and Busan were excluded from the monitoring plan of RGMN, however, they have the SIMN station if they abut onto the ocean. The depth of well in both networks generally ranges from 70 to 100 m. Each station has an automatic sensor that measures water level, temperature, and EC hourly. However, an additional sensor for temperature and EC is equipped for each station of SIMN to detect sea-water intrusion. Six RGMN and four SIMN stations were under operation around Pohang in February 2018.

The location maps and additional information on NGMS and RGMN/SIMN can be found on the website of each network: NGMS, <http://www.gims.go.kr/>; RGMN/SIMN, <http://www.groundwater.or.kr/>. And hourly precipitation data of Yangsan and Pohang weather stations were collected for plots for comparison (<http://www.weather.go.kr/>).



Figure S6. Location map of MW1 and the local groundwater monitoring stations. The distances between monitoring stations and MW1 are shown on the lines. The Yangsan stream runs southward on the right side of this figure, indicating the blue arrow. The map was edited from the location map provided by the National Groundwater Information Management and Service Center (GIMS) of Korea (<http://www.gims.go.kr/>).

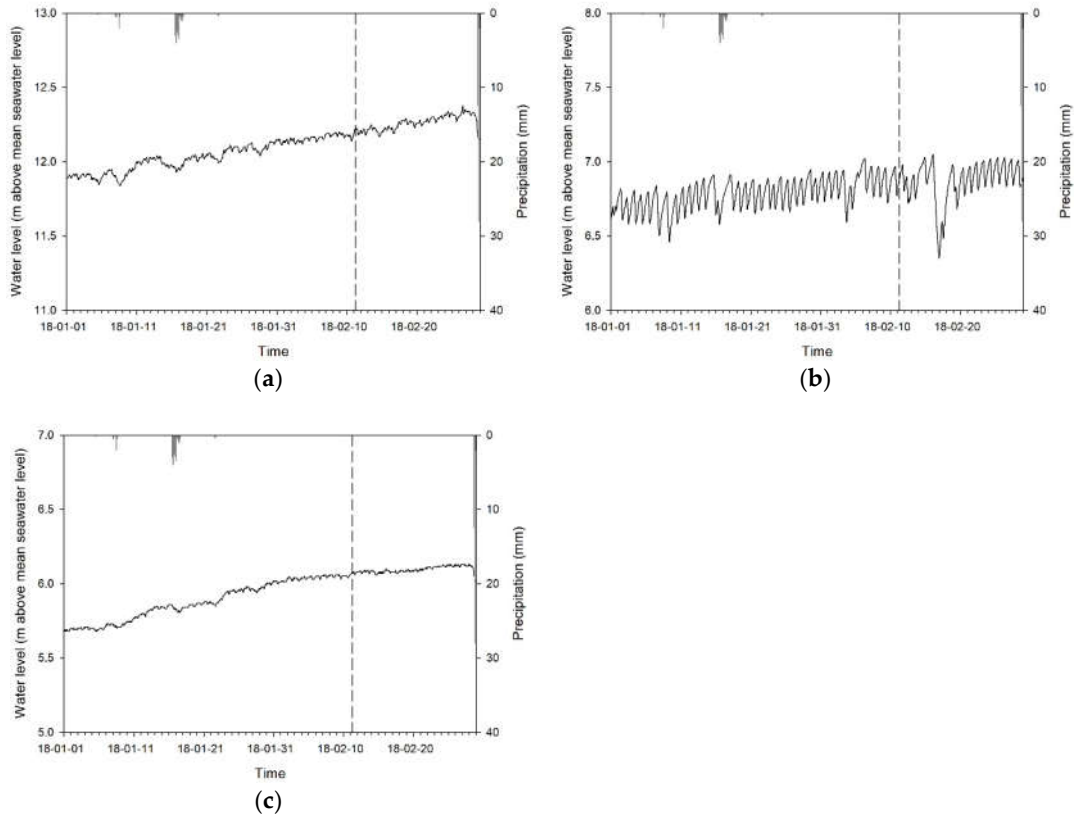


Figure S7. The water level fluctuations observed at (a) MG1, (b) MG2, and (c) MG3 stations between January 1, 2018, and February 28, 2018 (KST). The vertical dashed line indicates the occurrence time of the M4.6 earthquake.

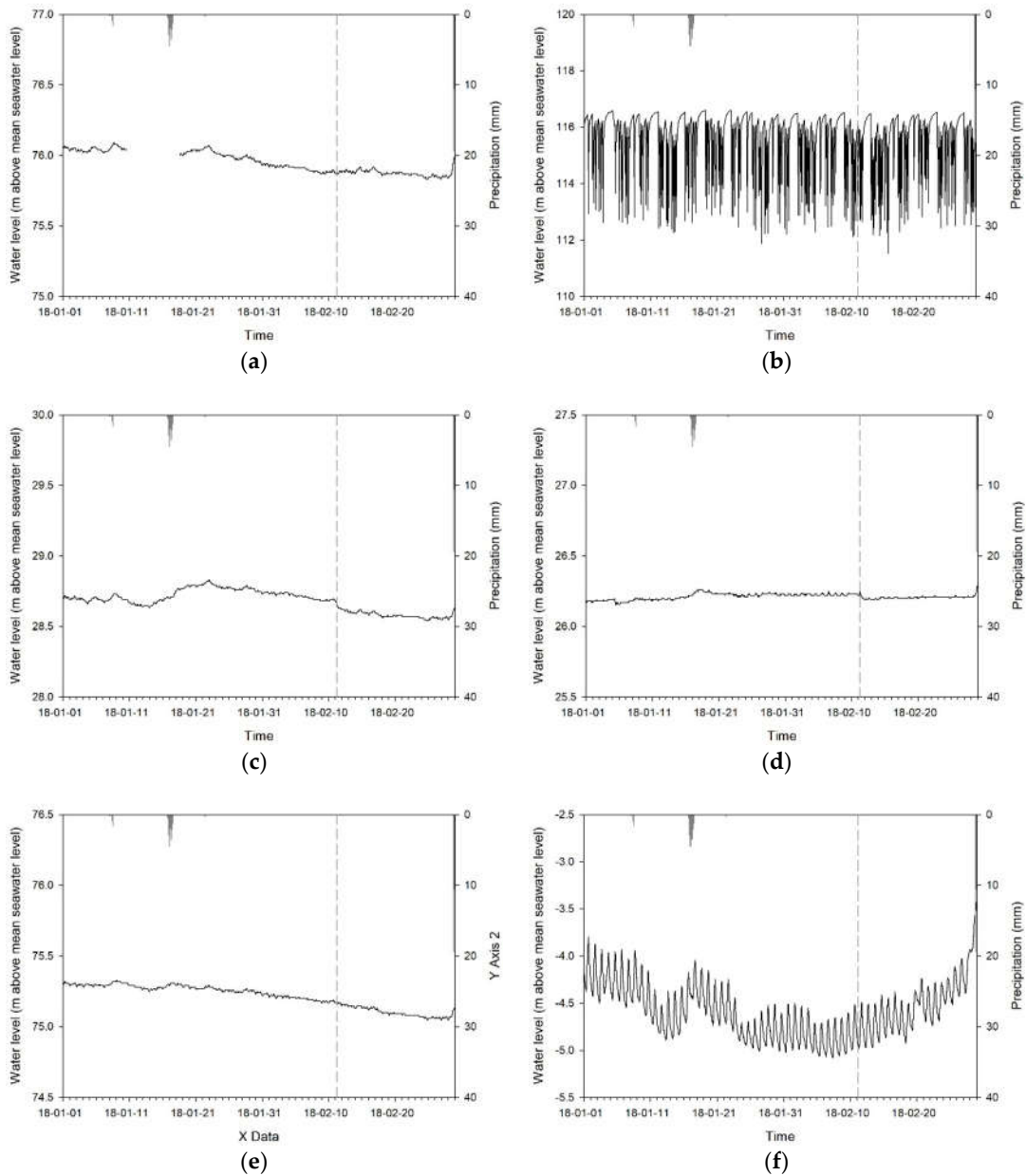
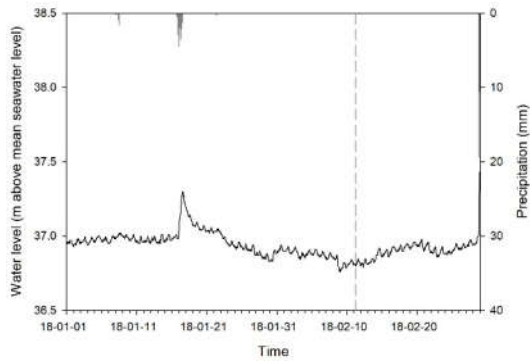
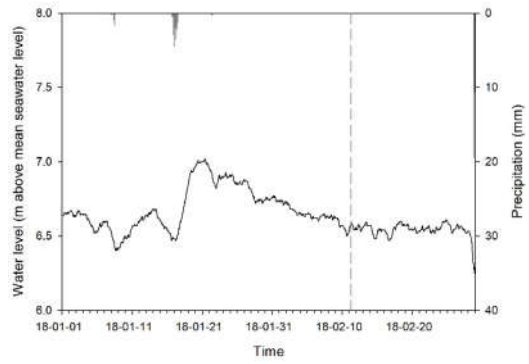


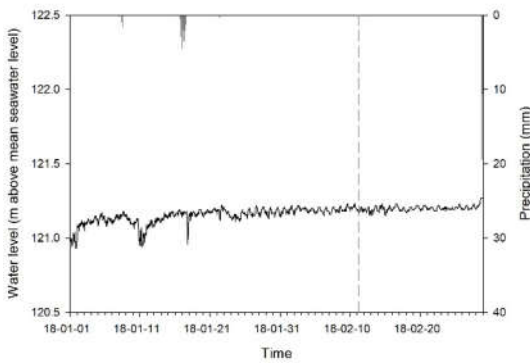
Figure S8. The water level fluctuations observed at (a) Pohang-Donghae, (b) Pohang-Gibuk, (c) Pohang-Guryongpo, (d) Pohang-Jangheung, (e) Pohang-Shingwang, and (f) Pohang-Yeonil stations of NGMN between January 1, 2018, and February 28, 2018 (KST). The vertical dashed line indicates the occurrence time of the M4.6 earthquake.



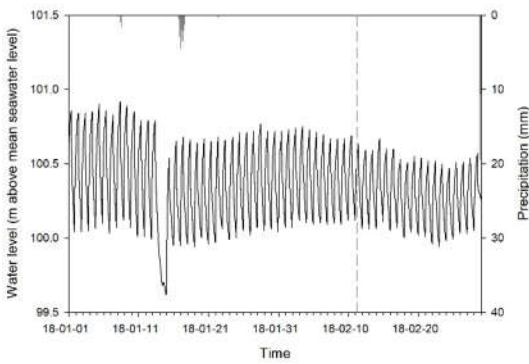
(a)



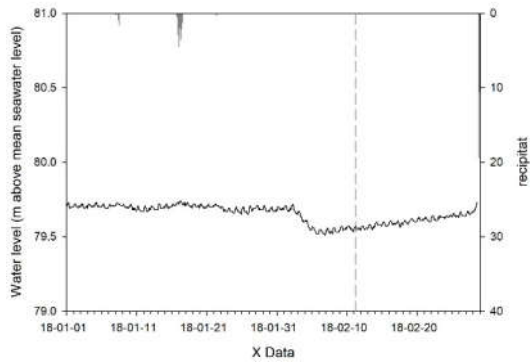
(b)



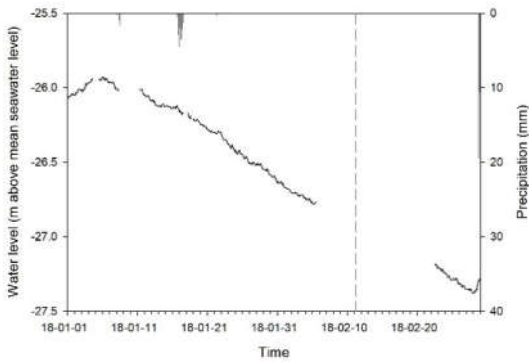
(c)



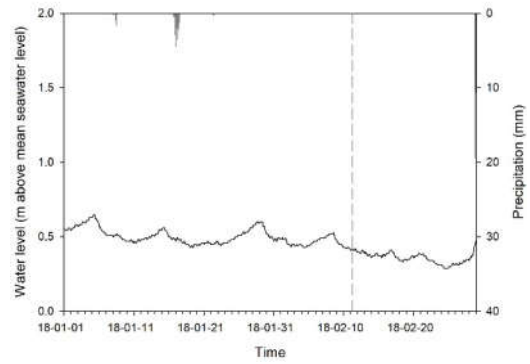
(d)



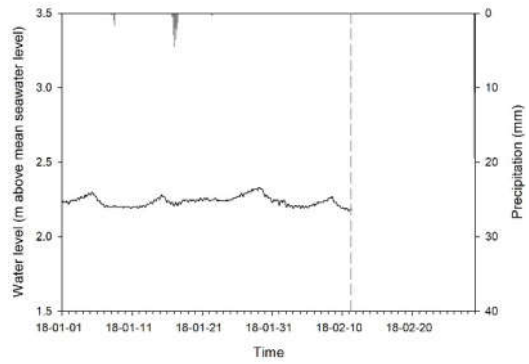
(e)



(f)



(g)



(h)

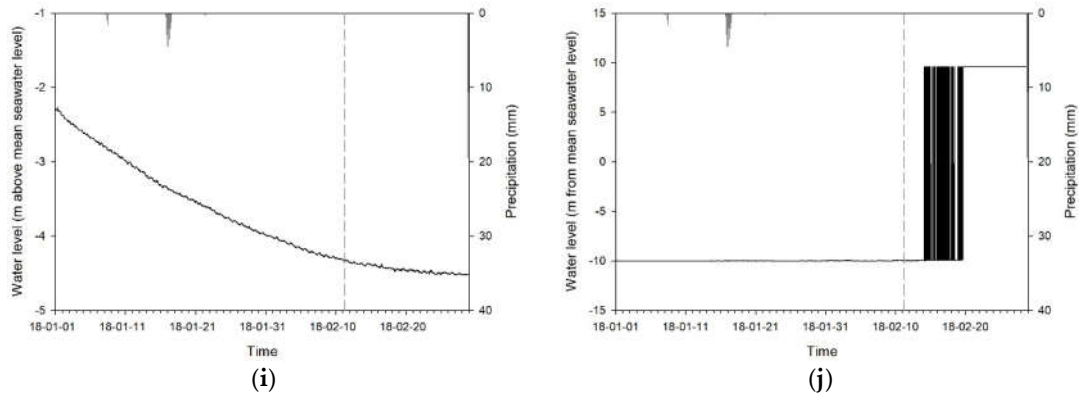


Figure S9. The water level fluctuation observed at (a) Pohang1 RGMN, (b) Pohang2 RGMN, (c) Pohang3 RGMN, (d) Pohang4 RGMN, (e) Pohang5 RGMN, (f) Pohang6 RGMN, (g) Gokgang1 SIMN, (h) Gokgang2 SIMN, (i) Yeonil1 SIMN, and (j) Yeonil2 SIMN stations between January 1, 2018, and February 28, 2018 (KST). The data of Gokgang2 The vertical dashed line indicates the occurrence time of the M4.6 earthquake. Please note that the data of Gokgang2 in this plot only contains the observation between 0 o'clock AM January 1 and seven o'clock AM February 11 (KST).